  Bull. Chem. Soc. Jpn., 57, 1169—1173 (1984)

On the Penetration Rate and the Role of Acids in the Control of Impregnation Profiles

Masaharu KOMIYAMA* and Robert P. MERRILL†
Department of Chemical Engineering, Faculty of Engineering, Tohoku University, Aramaki Aoba, Sendai 980
†*School of Chemical Engineering, Cornell University, Ithaca, New York 14853 U.S.A.*
(Recieved June 2, 1983)

Two factors which play important roles in determining the concentration profiles in the impregnation of porous catalysts, *viz.*, penetration rate of impregnating solution and the use of acids, were examined. The flow rate of impregnating solution into a spherical dry pellet consisting of polydispersed pores obeyed the equation which assumed constant pressure differential at the liquid front independent of its position in the pellet. The adsorption behavior of nickel ions onto γ-alumina strongly depended on the pH of the solution, and very weakly on the kind of acids used. By controlling the pH of the impregnating solution, it was possible to obtain a surface impregnation, a uniform impregnation and a subsurface impregnation for nickel on γ-alumina.

Many catalysts in common use are produced by impregnating a pellet of a porous support with a solution of catalyst precursors. During the impregnation and subsequent drying, small crystallites of the catalyst precursors are deposited on the internal surface of the support material. The mass transfer processes involved in the impregnation and drying steps typically do not reach equilibrium, resulting in non-uniform concentration profiles of impregnant along the radius of the support pellet. The importance of designing and/or controlling these concentration profiles, or impregnation profiles, has been recognized, because optimized impregnation profiles may bring about higher overall reaction rate,[1] better light-off performance,[2,3] longer catalyst life,[3,4] and/or conservation of expensive catalyst metals.[5,6]

In order to design and control the impregnation profiles the factors influencing the profiles must be identified by constructing appropriate impregnation models. The impregnation step involves the time-dependent flow of impregnating solution into a dry pellet and adsorption of impregnant onto the pore wall. The interior dispersal of impregnant during this step has been analyzed in detail by Vincent and Merrill,[7] for single-component impregnation using a single-pore model. Their analysis has since been expanded in two directions: models for single-component impregnation into a porous sphere[8] and the multi-component impregnation using the single-pore model[9] have been presented. This paper examines experimentally two aspects of these two developments.

The expansion of the single-pore model to a three-dimensional porous sphere is like the one-dimensional model based on the analysis of Washburn[10] who assumed a succession of Pourselle steady states. Its derivation involved an assumption, *viz.*, constant pressure differential at the liquid front independent of its position inside the pellet (*cf.* Fig. 1 (a)). Impregnation profiles calculated from this expanded model quantitatively agreed with experimental impregnation profiles,[8] although no theoretical or experimental basis for the assumption was presented. The dynamics of liquid uptake during catalyst impregnation is not well understood, and is at the stage of being closely examined.[11] In the first part of this paper we examine this process, by directly measuring the penetration rate of a liquid into a spherical pellet.

Kulkarni *et al.*[9] have expanded the single-component model to multi-component impregnation using the single-pore model of Vincent and Merrill[7] and assuming competitive adsorption among the impregnants. For the preparation of subsurface impregnation employing various acids, their model calculations were in qualitative agreement with some of the Pt/γ-alumina impregnation profiles reported by Shyr and Ernst,[12] although the sharp breakthroughs observed in Ni/γ-alumina subsurface impregnation profiles[8] (*cf.* Fig. 4) were not reproduced. This may be an indication that for this particular system the mechanism of producing subsurface impregnation by the use of acids may not by a simple competitive adsorption between the nickel ions and the acid species. The latter part of the present paper examines the mechanism of controlling impregnation profiles by the use of acids in the preparation of Ni/γ-alumina catalysts.

Experimental

Spherical γ-alumina pellets of about 4 mm-diameter supplied by Universal Oil Products were employed as the porous support. Their pretreatment and characterization are found elsewhere.[8] The poze size distribution of the alumina support is bimodal, with peak radii at around 2.5 nm (found by nitrogen adsorption) and in between 0.1 to 0.3 μm (observed by scanning electron microscopy, SEM).

The rate of 1-bromonaphthalene penetration into the alumina sphere was examined by using a light microscope with a calibrated eyepiece. 1-Bromonaphthalene was chosen as a model liquid because its refractive index of 1.66 is nearly the same with that of γ-alumina, which is 1.7. Thus alumina contacted with 1-bromonaphthalene becomes transparent, enabling one to observe through a light microscope the position of the penetrating liquid front as a function of time.

Effects of acids on nickel adsorption on γ-alumina were examined by aqueous phase adsorption measurements, which were carried out by soaking powdered (<65 mesh) alumina pellets into solutions of nickel nitrate with or without additives such as citric acid or hydrochloric acid. Adsorption experiments were performed in a constant-temperature bath at 20.0 °C with continuous stirring for 1 h. The temperature and the contact time were chosen to simulate the actual catalyst impregnation. After one hour the alumina powder

was separated from the solution by centrifuge, and the solution pH was measured. The amount of nickel ion adsorbed onto the solid surface was determined spectrophotometrically from the incremental loss of Ni(II) species in the liquid phase by adding an appropriate amount of KCN to the solution, thus converting nickel ion into a cyanide complex, and measuring its absorption at 310 nm.[13] Such a procedure was necessary in order to measure the small difference in nickel concentration caused by its adsorption on γ-alumina, because the absorption sensitivity of nickel aquo complex at around 400 nm was not sufficient to make reliable measurements.

A series of Ni/γ-alumina catalysts, designed to demonstrate the effects of pH on impregnation profiles, were prepared by impregnating alumina pellets with pH-adjusted aqueous solutions of nickel nitrate. Solution pH was adjusted by the addition of citric acid and/or ammonium hydroxide. Detailed procedures for the catalyst preparation are found elsewhere.[8] For the measurements of the impregnation profiles of the finished catalysts, a JEOL JXA 733 electron microprobe was employed. Detailes of sample preparation and procedure for this measurement are also presented elsewhere.[8]

Results and Discussion

Penetration Rate of Impregnating Solution. The three-dimensional impregnation model developed earlier,[8] which is an extension of a single-pore model proposed by Vincent and Merrill,[7] predicts the penetration rate of the liquid front into a spherical pellet by the following equation:

$$(1-\Gamma)^3 = 1-\tau^{1/2}, \qquad (1)$$

where Γ is the reduced radial position in a sphere, or one minus the fractional radius, and τ is the reduced time, or actual time divided by t_L which is the time necessary for the liquid to reach the center of the pellet. It was assumed[8] in deriving the above equation that the pressure differential is constant at the liquid front regardless of its position in the sphere. This assumption is depicted in Fig. 1 (a), where the pressure profiles along the radius of a pellet which is represented by a long single pore of the length of the pellet radius are shown for two positions of liquid front. Also note that pressure differential along the radius of the pellet at any given time is approximated by a linear function.

The validity of this assumption and its physical basis may become clearer by examining directly the actual rate of liquid penetration, or the front velocity of the penetrating liquid, and comparing it with the model prediction. Figure 2 shows measurements of the front positions of 1- bromonaphthalene penetrating into γ-alumina spheres as functions of time τ. Two sets of measurements are shown, which represent the upper and the lower bound of measurements among a number of pellets tested. The solid line in the figure was calculated by using the above Eq.(1) which is non-dimensionalized and thus is applicable to any liquid penetration. The model calculation agrees well with the measured front positions in the range of $\Gamma>0.3$. Where $\Gamma<0.3$, the actual Γ is larger than predicted. This results from very large initial front velocities followed by a period of near zero velocity.

In order to interpret these results consider first a pellet consisting of monodispersed pores, for which

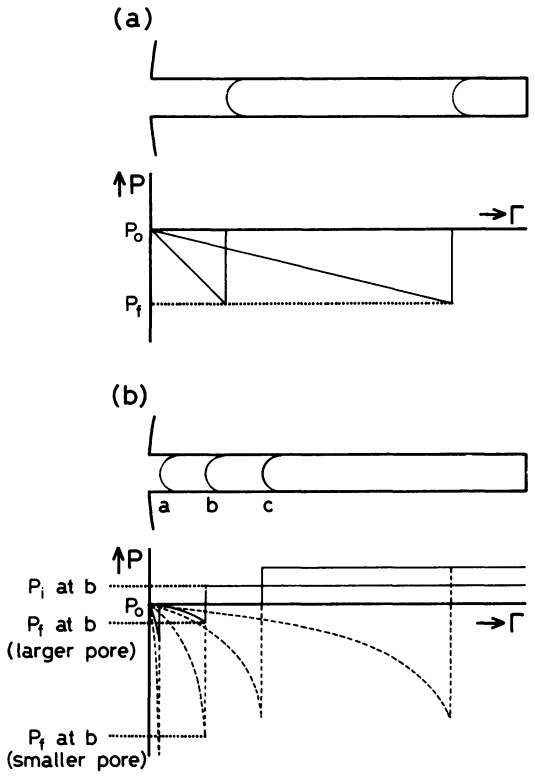

Fig. 1. Pressure profiles in the impregnating solution along the radius of a pellet.
(a) Model profile assumed in the three-dimensional impregnation model; (b) profile concieved from the results of the liquid penetration measurements. Solid lines: larger pores. Broken lines: smaller pores. P_i: Pressure inside the pellet; P_o: pressure outside the pellet; P_f: pressure at the liquid front.

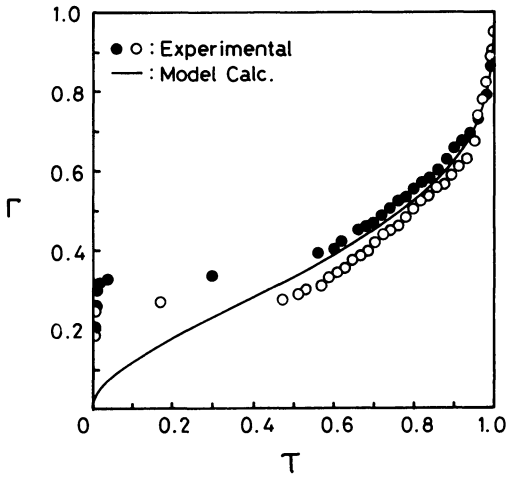

Fig. 2. Non-dimensionalizad penetration depth, $\Gamma = z/L$, of 1-bromonaphthalene into γ-alumina pellet as a function of non-dimensionalized time, $\tau = t/t_L$. Open and closed circles: experimental; solid line: model calculation using Eq. (1).

pressure profiles along the radius of the pellet at various times are represented by solid lines in Fig. 1 (b). For each profile there is a monotonic decrease in pressure up to the meniscus of the liquid front followed by a

discontinuous increase across the meniscus. At the onset of impregnation (point **a** in Fig. 1 (b)), the pressure inside the pellet, P_i, is similar to that outside the pellet, P_o, and the liquid penetrates with the capillary pressure, $(P_i-P_f)\simeq(P_o-P_f)$, as driving force. As the liquid progresses (point **b**), it compresses the air inside the pellet, raising P_i higher than P_o. Since the pressure drop at the liquid front, (P_i-P_f), is fixed for a given pore-liquid system, this higher P_i results in smaller driving force, (P_o-P_f), slowig down the rate of liquid penetration. Penetration will be stopped when P_i is balanced with the capillary pressure, *i.e.*, $P_o=P_f$ (point **c**) and the driving force for flow is zero.

In the case of a pellet consisting of polydispersed pores, such as the present one, the situation will be more complicated. At the early stage of impregnation liquid is mainly carried into the pellet through larger pores which have higher mass flow than smaller pores.[7,8] The flow through these larger pores will eventually be stopped by the process discussed above. The data in Fig. 2 indicate that this happens at $\Gamma\simeq0.3$, which gives P_i of about 3 atmosphere. This corresponds to the capillary pressure of the pores with radius of about 0.7 μm, which is in the larger end of the pore size distribution observed by SEM.

Even after liquid in the larger pores is halted, however, liquid in smaller pores, with pressure profiles represented by the broken lines in Fig. 1 (b), advance due to the higher capillary pressure. Volume occupied by this advancing liquid will be compensated by a receding meniscus in larger pores, keeping P_i constant. As a consequence liquid in larger pores is slowly pushed back, eventually making the pores empty to serve as air-escape channels. In the present system this is a long process as seen from the flat portion of the measured liquid front positions in Fig. 2, *i.e.*, the region where the observed velocity of the front is zero. Note that the wavelength of white light, which was used in the microscope, peaks above 1 μm so that neither the receding meniscus in larger pores nor the advancing meniscus in the smaller pores can be detected. The opening of the air channels is confirmed by air bubbles which are observed to form at the exterior of pellet at *ca.* $\tau=0.5$. Once the air channels are established, P_i will be kept constant at this level by advancing liquid to keep the channels open. Since the pressure drop at the liquid front is fixed for a given liquid-pore system, constant P_i means constant P_f, fulfilling the assumption described above.

It follows from the above discussion that there are two limiting cases in which the assumption of constant P_f holds. One is the early stage of impregnation (*e.g.*, point **a**), where $(P_o-P_f)\simeq(P_i-P_f)$. In this case (P_i-P_o) could be neglected compared to the driving force, (P_o-P_f), and P_f holds approximately constant. Note that this limiting case would dominate the impregnation process if a support consisting of very small pores is used. The pressure balancing in such system would not occur until very late in the impregnation process, *i.e.*, point **c** for example in Fig. 1 (b), which is displaced close to $\Gamma=1$. The other limiting case is the later stage of impregnation, where P_f is kept constant by the mechanism discussed above. Also note here that if a support consisting of relatively large pores is used, the pressure balancing would occur very early stage in the impregnation, *i.e.*, point **c** is displaced close to $\Gamma=0$, and this limiting case will dominate the impregnation. These two limiting cases are obvious in the data shown in Fig. 2, where early stage ($\tau=0$—0.03) corresponds to the former case and later stage ($\tau=0.4$—1) to the latter case. At intermediate level ($\tau=0.03$—0.4) during which either limit is appropriate, there is a transition from the larger pore-dominated region to the smaller pore region.

Effects of Acids on the Adsorption Behavior of Nickel. The effect of nitric acid addition on nickel ion adsorption on γ-alumina powder has already been reported.[8] Its results showed that the amount of nickel ion adsorbed during one hour of contact time is strongly influenced by the pH of the solution. Nickel adsorption on γ-alumina was shown to be inhibited below a pH of about 4, and the amount of nickel adsorption abruptly increased at around a pH of 5.2. The adsorption continuously increased past the pH of pure nickel salt solution to the basic side. While such adsorption behavior was presumed to be a pH effect rather than an example of competitive adsorption, and methods of preparing subsurface impregnation utilizing this pH effect has been demonstrated,[8] these results were not conclusive since it used only one acid species and there still remains the possibility that competitive adsorption of some form is still operative.[9]

In Fig. 3 adsorption as a function of pH is plotted for a number of other acids commonly used to prepare subsurface impregnation of Ni/γ-alumina. In order to simplify the presentation, data points for hydrochloric acid and glicine are replaced by lines connecting through them in the figure, since the scatter in the adsorption data was very small for those acids. Plotted in the figure is the final pH of the solution measured after alumina powder was separated by a centrifuge. It shows that regardless of the kind of acid added to the solution, nickel adsorption abruptly increases at a pH of about 5.2. These results support the previous discussion[8] that nickel adsorption on γ-alumina surface is

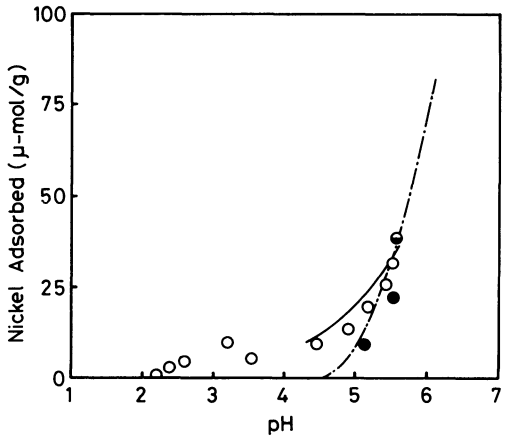

Fig. 3. The effect of pH on $Ni(NO_3)_2$ adsorption on γ-alumina. Initial concentration of $Ni(NO_3)_2$: 0.00988M. Contact time: 1h. Plotted pH are those after the contact. Additives: none (◒), citric acid (○), oxalic acid (●), hydrochloric acid (——), glycine (—·—).

controlled by the pH of the solution and not by competitive adsorption. The kind of acid species used to control pH seems to have little effect on the extent of adsorption.

A close examination of Fig. 3 shows, however, that the acids can be grouped into two types: One that inhibits nickel adsorption completely below pH of about 4, and another that allows weak adsorption even below that pH. Nitric acid,[8] oxalic acid, and glicine belong to the former while citric and hydrochloric acids belong to the latter.

This work is not intended to elucidate the physical chemistry of the pH effect. Some possible explanations have been suggested previously.[8] A detailed discussion on pH-dependent adsorption of metal cations onto oxide surfaces is given by Brunell.[14] Here we concentrate on the utilization of this pH effect for the control of impregnation profiles.

pH-Controlled Catalyst Impregnation. The strong effect of pH upon the amount adsorbed provides a degree of freedom in controlling the concentration profiles in the impregnation of porous catalysts. By exploiting these effects subsurface, uniform and/or surface impregnation can be produced.

The preparation of subsurface impregnation, through manipulating pH, has been demonstrated[8] for Ni/γ-alumina system using nitric acid as pH controller. The effects of concentrations of nitric acid and nickel salt were examined and discussed in detail.[8] When a support immersed in an impregnating solution of low pH, cation adsorption on the pore wall is inhibited at first. If the pH controlling species is adsorbed on the pore wall, then as the solution penetrates the pore its local pH gradually increases. At some point along the axis of the pore the pH may increase to the point where adsorption of the co-impregnated metal cation becomes appreciable. This should result in an outer shell of metal free adsorbate and a subsurface impregnation past the point where the critical pH is achieved, provided that molecular diffusion along the axis of the pore is small enough.

Figure 4 compares the nickel concentration profile of a sample using nitric acid (profile **a**) and citric acid (profile **b**) to suppress adsorption at the exterior of the pellet. In these plots the nickel concentration, determined by X-ray fluorescence, is presented as a function of fractional radius. A value of 1.0 in the radius represent the exterior of the pellet. In profile **b** the open circles are for pellets sectioned after drying and the solid circles are for pellets sectioned before drying. It is clear in profile **b** that the surface enhanced concentration is due to segregation during drying,[8] and therefore not pertinent to this discussion of the impregnation step.

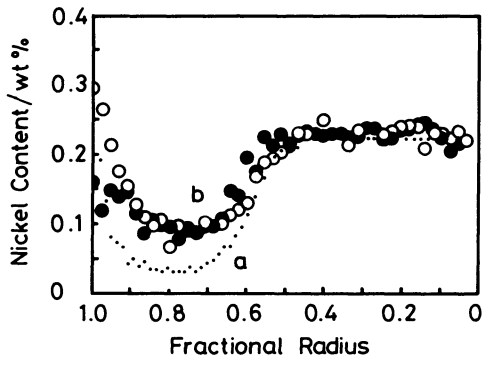

Fig. 4. Nickel subsurface impregnation produced by using nitric acid (profile **a**, dotted line) and citric acid (profile **b**, open and closed circles) as pH controller. Initial concentrations: $Ni(NO_3)_2$, 0.0247 M (1 M= 1 mol dm^{-3}); HCl, 0.000982 M; citric acid, 0.0012 M.

Profiles **a** and **b** are very similar to each other, indicating that both acids play almost identical roles, *i.e.*, pH control, in producing subsurface impregnation.

Two minor differences are noted between these two profiles. First, the acid concentration necessary to create the same thickness for the low metal loading band (fractinal radius>0.6) is higher for citric acid than for nitric acid. This is understood from the above pH-controlled impregnation mechanism, which assumes that the nickel adsorptivity is controlled by local pH. Since the dissociation constant of citric acid is much lower than that of nitric acid, a higher concentration of citric acid is necessary in order to obtain the same pH profile along the radius of the pellet and thus to create the similar nickel concentration profiles. Second, the amount of nickel deposition at the low loading region (0.9>fractional radius>0.6) is higher when citric acid was used as pH-controller than when nitric acid was used. In case of profile **a** in Fig. 4 the deposition in this region was considered to be produced by the overlap of the leading edge of the breakthrough and the tail of the surface-segregated deposition band. A higher loading in the surface region for profile **b** is attributed to the low but non-negligible adsorption below pH=4 for citric acid-controlled adsorption (*cf.* Fig. 3). In contrast to nitric acid,[8] citric acid does not completely inhibit the adsorption of nickel ions in the region where pH of the penetrating solution is still low.

It is expected from the results presented in Fig. 3 and the mechanism of pH-controlled subsurface impregnation deduced from it, that it may also be possible to produce a profile with a high concentration at the surface of the pellet if the pH of the impregnating solution is adjusted to higher side where adsorptivity enhancement is observed instead of inhibition (see Fig. 3). Presented in Fig. 5 are the nickel concentration profiles of the samples impregnated with solutions of varying initial pH. The same concentrations of nickel nitrate and citric acid were employed for all samples in Fig. 5 as well as the sample in Fig. 4, profile **b**, The initial pH was adjusted by adding an appropriate amount of ammonium hydroxide to the solution. Only the initial value of pH is presented in the figure, since it is not possible to determine experimentally the final pH of the solution in the pore at the end of the impregnation. As a control, single-component impregnation was also performed and the resulting profile is shown in Fig. 5 (sample No. F-1). Note that there is no evidence of significant surface segregation in any of these samples. There is no disparity between closed and open circles.

Nickel nitrate at this concentration produces a uniform impregnation profile as shown in Fig. 5, control sample No. F-1. When the initial pH was adjusted to

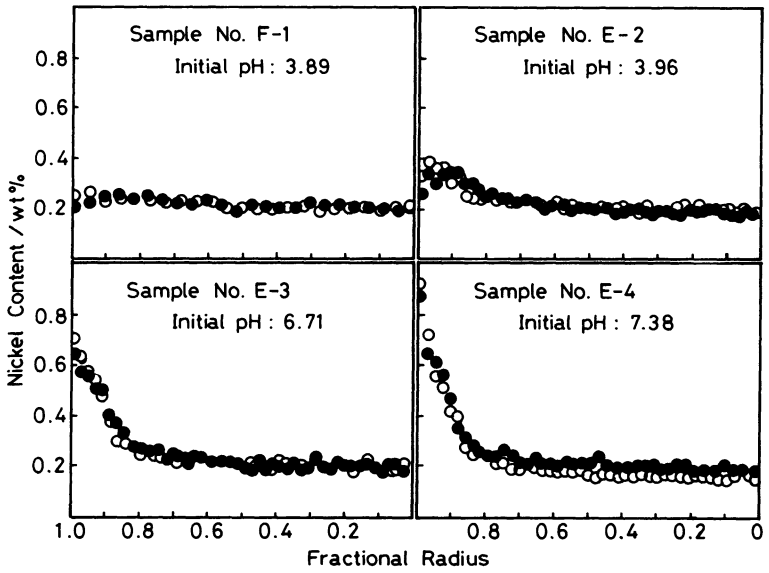

Fig. 5. Nickel concentration profiles impregnated at various initial pH.

the acidic side where adsorption inhibition occurs, subsurface impregnation was produced as discussed above (Fig. 4, profile **b**). When the starting pH was adjusted to higher side where nickel adsorption is enhanced, surface impregnation profiles resulted (Fig. 5, sample Nos. E-2 through E-4). Note that the higher the initial pH of the solution, the larger the nickel concentration near the outer surface of the pellet. The mechanism is exactly the same as that which produced subsurface impregnations except that adsorption enhancement occurs near the external surface of the pellet instead of inhibition.

While this pH effect adds another degree of freedom in engineering impregnation profiles, it also adds complication to the modeling of the impregnation process. Major parameters which play important roles in determining impregnation profiles involve characteristics of metal cation adsorptivity such as maximum amount of adsorption or an adsorption rate coefficient.[7] The consequence of the above pH effect is the dependence on local pH of these otherwise constant parameters. Models for the pH-controlled impregnation must consider these parameters as functions of local pH of the solution in the pore, which depends both on Γ and τ. It is not surprising, therefore, that models describing inhibition *via* competitive adsorption[9] do not predict the sharpness of the concentration.

For subsurface impregnation (acidic side pH control) using nitric acid, the pH effect was represented as a step function,[8] *viz.*, complete inhibition below pH=5.2 and single component behavior above that pH. Such an approach was justified because with this acid the pH dependence of nickel adsorption can be closely approximated by a step function, and also because of the resulting good agreement between the actual impregnation profiles and the ones calculated using this approximation, as reported earlier.[8] Such a treatment, however, may not be appropriate for the case of higher side pH control or acidic side control using acids like citric acid, because the nickel adsorption behavior for these cases cannot be approximated by a step function of pH. Further work is necessary in order to formulate an impregnation model incorporating such pH effects.

The work is partially supported by the Grant for Scientific Research No. 57750699 from the Japanese Ministry of Education, Science and Culture.

References

1) R. W. Maatman, *Ind. Eng. Chem.*, **51**, 913 (1959).
2) E. R. Becker, and J. Wei, *J. Catal.*, **46**, 365 (1977).
3) L. L. Hegedus, J. C. Summers, J. C. Schlatter, and K. Baron, *J. Catal.*, **56**, 321 (1979).
4) E. R. Becker, and J. Wei, *J. Catal.*, **46**, 372 (1977).
5) S. Minhas, and J. J. Carberry, *J. Catal.*, **14**, 270 (1969).
6) T. G. Smith, and J. J. Carberry, *Can. J. Chem. Eng.*, **53**, 347 (1975).
7) R. C. Vincent, and R. P. Merrill, *J. Catal.*, **35**, 206 (1974).
8) M. Komiyama, R. P. Merrill, and H. F. Harnsberger, *J. Catal.*, **63**, 35 (1980).
9) S. S. Kulkarni, G. R. Mauze, and J. A. Schwarz, *J. Catal.*, **69**, 445 (1981).
10) E. W. Washburn, *Phys. Rev.*, **17**, 273 (1921).
11) S. -Y. Lee, and A. Aris, "Preparation of Catalysts III," ed by G. Poncelet, P. Grange, and P. A. Jacobs, Elsevier, Amsterdam (1983), p. 35.
12) Y. S. Shyr, and W. R. Ernst, *J. Catal.*, **63**, 425 (1980).
13) T. M. Florence, *Anal. Chim. Acta*, **19**, 548 (1958).
14) C. P. Brunell, "Preparation of Catalysts II," ed by B. Delmon, P. Grange, P. Jacobs, and G. Poncelet, Elsevier, Amsterdam (1979), p. 51.